geoconvention
Virtual Event
September 21-23
2020
CSPG · CSEG · CWLS · GAC · MAC · IAH

# Full waveform inversion of distributed acoustic sensing strain data

*Matthew V. Eaid, Scott Keating, Kris A. Innanen*
*University of Calgary, CREWES Project*

## Summary

Distributed acoustic sensing (DAS) has become an important tool for seismic data acquisition. Utilizing optical fibers, DAS senses the strain induced by propagating seismic wavefields. The noninvasive nature of these fibres allows for their placement in monitoring wells, hydraulic fracture treatment wells, and producing wells, expanding the reach of downhole sensor technologies. The acquisition geometries that DAS affords, supply supplemental and complementary data to conventional surface geophone surveys. Inclusion of DAS data in FWI holds the potential to greatly improve estimates of subsurface parameters, especially during hydraulic fracturing, cyclic steam stimulation, and SAGD. To date little work has focused on the use of DAS data in FWI. Most of the methods that have been developed rigidly assume a straight fibre in a vertically oriented well. Here we present a novel method for the inversion of the strain data supplied from DAS fibres of arbitrary geometry. Our method is also powerful in its ability to simultaneously invert geophone and DAS data without altering the form of the gradient.

## Theory

Conventional full waveform inversion (FWI), pioneered by Tarantola (1984, 1986) is a powerful tool for high resolution estimates of subsurface properties. The goal of FWI is the estimation of a model of subsurface parameters that reduces discrepancies between modeled data **Ru** and observed data **d**, by considering a constrained optimization problem of the form

$$\min_{\mathbf{m}} \frac{1}{2}\|\mathbf{Ru}-\mathbf{d}\|_2^2 \quad \text{subject to} \quad \mathrm{S}\mathbf{u}=\mathbf{f}. \tag{1}$$

Equation (1) is constrained by the requirement that it satisfies the wave equation, where S is the wave equation operator – here for the isotropic elastic wave equation – and **f** is the source function. Optimization problems of this type are commonly solved through gradient-based methods to provide an estimate of the subsurface model parameters **m.** The gradient for this problem, solved for through Lagrange multipliers and the adjoint state method is,

$$\frac{\partial \phi}{\partial \mathbf{m}} = \left\langle \frac{\partial \mathrm{S}}{\partial \mathbf{m}}\mathbf{u}, \lambda \right\rangle. \tag{2}$$

The gradient in equation (2) can be interpreted as the cross-correlation of a scaled version of the forward modelled wavefield **u**, and an adjoint wavefield $\lambda$ computed through solution to the adjoint wave equation below,

$$\mathrm{S}^{\dagger}\lambda = \mathbf{R}^{\mathrm{T}}(\mathbf{Ru}-\mathbf{d}). \tag{3}$$

In the preceding discussion, the matrix $\mathbf{R}$ is used to incorporate properties of the receivers in computing the modelled data from the modelled wavefield. Conventionally, when considering geophone data, matrix $\mathbf{R}$ performs the function of sampling the appropriate portion of the displacement wavefield at the locations of the receivers. However, it is important to note that the form of $\mathbf{R}$ does not alter the form of the objective function. Additionally, because the receiver matrix $\mathbf{R}$ is independent of the model parameters $\mathbf{m}$, its form does not influence the expression for the gradient. The form of $\mathbf{R}$ is therefore free to change without affecting the form of the gradient or objective function, allowing it to incorporate properties of receivers such as those of a DAS fibre.

Distributed acoustic sensors are sensitive to the strain induced by seismic waves along the tangential direction of the fibre. To model the data they supply, first the strain field is computed through a finite difference approximation to the expression for a strain tensor. The rank 2 strain tensor is then projected onto the coordinate system of the fibre and the tangential component ($\epsilon_{tt}$) is extracted. Following this procedure, the expression for the response of a DAS fibre can be expressed as,

$$\epsilon_{tt} = \left(\hat{\mathbf{t}} \cdot \hat{\mathbf{1}}\right)^2 \epsilon_{xx} + 2\left(\hat{\mathbf{t}} \cdot \hat{\mathbf{1}}\right)\left(\hat{\mathbf{t}} \cdot \hat{\mathbf{3}}\right)\epsilon_{xz} + \left(\hat{\mathbf{t}} \cdot \hat{\mathbf{3}}\right)^2 \epsilon_{zz} \tag{4}$$

where $\hat{\mathbf{t}}$ is a unit vector in the direction of the fibre tangent, $\hat{\mathbf{1}}$ and $\hat{\mathbf{3}}$ are Cartesian unit vectors, and $(\epsilon_{xx}, \epsilon_{xz}, \epsilon_{zz})$ are the Cartesian components of strain in two dimensions. To invert data from DAS fibres, we construct $\mathbf{R}$ to handle the procedure required to turn the displacement wavefield $\mathbf{u}$ into DAS data $\epsilon_{tt}$. Specifically, $\mathbf{R}$ computes the strain field from the displacement field, projects this strain field onto the coordinate system of the fibre and invokes what is known as gauge length sampling by averaging the DAS response over one finite difference cell. Importantly, the method presented here is flexible in its ability to incorporate strain data from arbitrarily complex fibre shapes. Additionally, because the form of the objective function in equation (1), and the gradient in equation (2) are the same for geophone and DAS data, a version of $\mathbf{R}$ can be constructed to simultaneously invert geophone and DAS data.

### *Fibre sensitivity*

The response of a DAS fibre to a propagating wavefield in equation (4) is the weighted sum of the components of the Cartesian strain field. The weights are dependent on the geometry of the fibre and express the sensitivity of a given fibre geometry to each component of the strain field. The work that has considered FWI of DAS strain data usually considers a straight fibre in vertically oriented wells. Fibres of this type have a vertically oriented tangent, lacking sensitivity to the $\epsilon_{xx}$ and $\epsilon_{xz}$ components of strain. Fibres can be made more sensitive to the other components of the wavefield through shaping them in more complex geometries, such as helices (Innanen, 2017). An important consideration is how the geometric shape of the fibre and its resulting sensitivity affects parameter estimates from FWI.

For example, a straight fibre in a horizontal well is only sensitive to the $\epsilon_{xx}$ component of strain. However, for explosive surface sources a significant portion of the strain field sensed by the buried fibre consists of $\epsilon_{zz}$ strains. We are now left with a choice: do we choose a straight fibre

in which we have certainty about what we measure - knowing that the fibre response is only influenced by $\epsilon_{xx}$ strains – but no sensitivity to a large portion of the wavefield, or do we shape this fibre to enhance its sensitivity to other portions of the wavefield, but reduce the certainty about which portions of the Cartesian strain field we measure? To answer this question, we investigate the effect of the fibre shape on the recovery of subsurface parameters in an FWI framework.

## Numerical Examples

To understand the effect of fibre geometry on parameter estimation we investigate a numerical example. For this example, we consider an acquisition geometry of explosive surface sources and a DAS fibre in a horizontal well. Inversions are performed for five different fibre geometries to examine the effect varying the geometry has on the quality of parameter estimates for $v_p$, $v_s$, and $\rho$. Figure 1 shows the results of inverting a simple toy model using these five fibre geometries and provides valuable insight into the effect fibre geometries have on parameter estimates. The first row shows the parameter estimates for density ($\rho$) in column 2, p-wave velocity ($v_p$) in column 3, and s-wave velocity ($v_s$) in column 4. Rows two through four show parameter estimates for helical fibres with wind angles of 54.7 degrees, 35 degrees, and 19.5 degrees. The final geometry that is considered here is a hybrid helical fibre consisting of two different wind rates, in this case sections of four and a half winds of 19.25-degree fibre connected by half winds of 59.5-degree fibre. With a long gauge length relative to the fibre wind, hybrid designs of this type benefit from having a relatively large sensitivity to the $\epsilon_{xz}$ component. Fibres that are symmetric about their central axis, including straight and helical fibres, can be shown to lack sensitivity to the shear strain ($\epsilon_{xz}$) component of the wavefield.

These results highlight the effect of fibre geometry on inversion results. All five fibre geometries provide poor estimates of density, that are heavily contaminated by noise, due to a lack of information carried about density by wavefields at transmission angles. However, the fibre geometries in row one, two, and four provide more resolved estimates than the other two geometries, highlighting the effect of geometry on parameter estimate. All five fibre geometries provide similar estimates of the p-wave velocity, with only minor differences between them. The major variance occurs in the parameter estimation of s-wave velocity. The straight fibre (row 1), 54.7-degree fibre (row 2), and 19.5-degree fibre (row 4) provide good, resolved, estimates of $v_s$. The hybrid fibre provides the most resolved estimate of $v_s$, benefitting from its enhanced sensitivity to $\epsilon_{xz}$. Interestingly, the 35-degree fibre (row 3), which is balanced in its sensitivity to $\epsilon_{xx}$ and $\epsilon_{zz}$ provides a poor estimate of $v_s$ relative to the other fibres. This result can be understood by evaluating equation 4. A fibre with equal sensitivity to $\epsilon_{xx}$ and $\epsilon_{zz}$ and no sensitivity to $\epsilon_{xz}$ results in a fibre that senses the dilatational component of the wavefield and is therefore shear wave blind. Information about $v_s$ for fibres of this type is likely gained through AVO effects.

## Conclusions

The work presented here provides a sandbox for the appraisal of different fibre geometries and their effect on inversion results. Using these tools allows for the design of fibres tailored for specific applications. For example, the fibre best situated to help delineate a steam chamber during SAGD or CSS, may not be the best fibre to use for the recovery of a baseline model for

4D projects. Use of tools of the type shown here can aid decisions on the optimal fibre geometry and improve the data supplied by DAS.

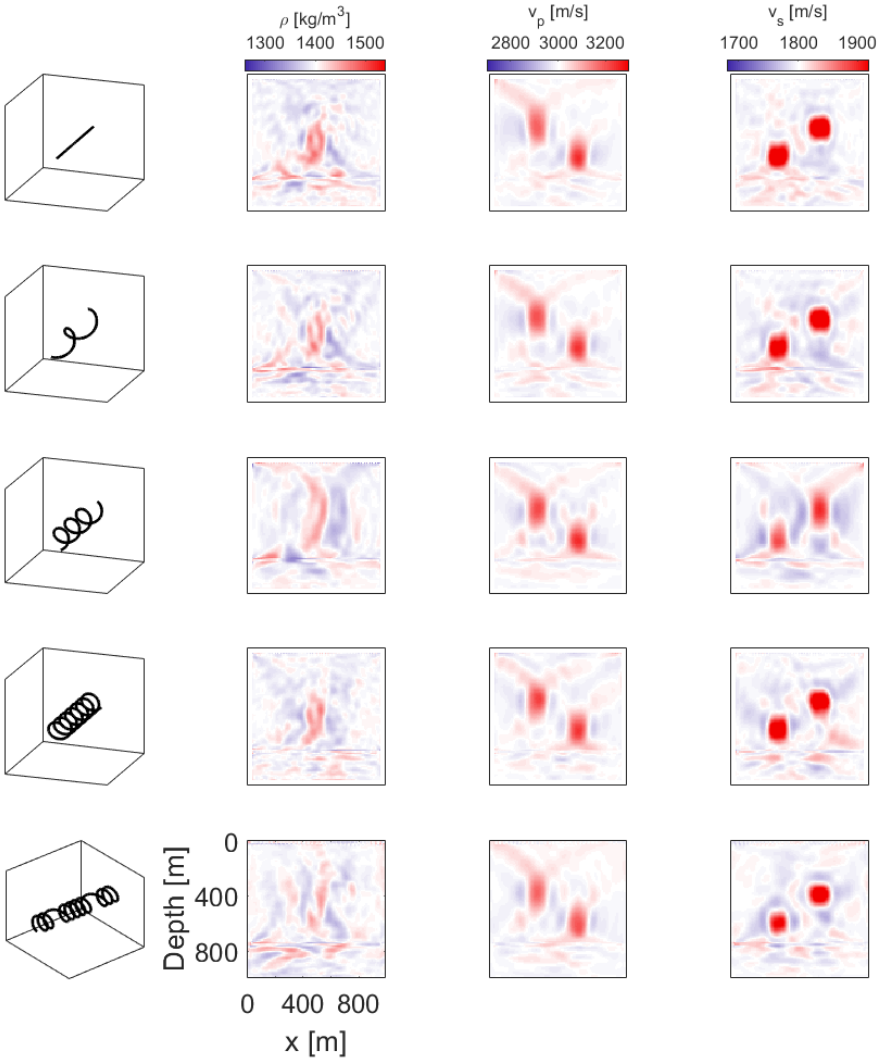


FIG 1: Inversion results for density (column 2), p-wave velocity (column 3), and s-wave velocity (column 4) from five fibre geometries. Column 1 shows sections of the fibre, highlighting the variance in geometry. Row 1 shows the inversion results for commonly deployed, straight fibres. Rows 2 through 4 show the inversion results for helical fibres with wind angles of 54.7 degrees, 35 degrees, and 19.5 degrees. Row 5 shows the inversion results obtained from data supplied by a hybrid helical fibre consisting of 4.5 winds of 19.25-degree fibre connected by half winds of 59.5-degree fibre.

## Acknowledgements

The authors would like to thank the sponsors of the CREWES project as well NSERC under the grant CRDPJ 461179-13 for making this work possible through their financial support. Matt Eaid and Scott Keating were partially supported through scholarships from the SEG Foundation.

### References

Innanen, K., 2017, Determination of seismic tensor strain from HWC-DAS cable with arbitrary and nested-helix winds, SEG Extended Abstracts, 926-930.

Tarantola, A., 1984, Inversion of seismic reflection data in the acoustic approximation, Geophysics, **49**, No. 8, 1259-1266.

Tarantola, A., 1986, A strategy for nonlinear inversion of seismic reflection data, Geophysics, **51**, 1893-11903.